Preprint
UCRL-JC-135292

Observation of Secondary Plasma Waves in Laser-Plasma Interaction Experiments

S. Depierreux, C. Labaune, H.A. Baldis, J. Fuchs and A. Michard

*This article was submitted to
First International Conference on Inertial Fusion Sciences and Applications
Bordeaux, France
September 12-17, 1999*

U.S. Department of Energy

Lawrence
Livermore
National
Laboratory

December 8, 1999

Approved for public release; further dissemination unlimited

DISCLAIMER

This document was prepared as an account of work sponsored by an agency of the United States Government. Neither the United States Government nor the University of California nor any of their employees, makes any warranty, express or implied, or assumes any legal liability or responsibility for the accuracy, completeness, or usefulness of any information, apparatus, product, or process disclosed, or represents that its use would not infringe privately owned rights. Reference herein to any specific commercial product, process, or service by trade name, trademark, manufacturer, or otherwise, does not necessarily constitute or imply its endorsement, recommendation, or favoring by the United States Government or the University of California. The views and opinions of authors expressed herein do not necessarily state or reflect those of the United States Government or the University of California, and shall not be used for advertising or product endorsement purposes.

This is a preprint of a paper intended for publication in a journal or proceedings. Since changes may be made before publication, this preprint is made available with the understanding that it will not be cited or reproduced without the permission of the author.

This report has been reproduced
directly from the best available copy.

Available to DOE and DOE contractors from the
Office of Scientific and Technical Information
P.O. Box 62, Oak Ridge, TN 37831
Prices available from (423) 576-8401
http://apollo.osti.gov/bridge/

Available to the public from the
National Technical Information Service
U.S. Department of Commerce
5285 Port Royal Rd.,
Springfield, VA 22161
http://www.ntis.gov/

OR

Lawrence Livermore National Laboratory
Technical Information Department's Digital Library
http://www.llnl.gov/tid/Library.html

UCRL-JC-135292

Observation of secondary plasma waves in laser-plasma interaction experiments

S. Depierreux[1], C. Labaune[1], H. A. Baldis[2], J. Fuchs[1], A. Michard[1]

[1]*Laboratoire pour l'Utilisation des Lasers Intenses, Ecole Polytechnique, CNRS, CEA, 91128 Palaiseau cedex, France*
[2]*Institute for Laser Science and Applications (ILSA)*
Lawrence Livermore Laboratory, POB 808, Livermore CA 94550, USA

Abstract

An experiment is described where the two products of the Langmuir Decay Instability (LDI) of a primary electron plasma wave have been observed and identified without any ambiguity. Primary Langmuir waves are driven by Stimulated Raman Scattering (SRS) of an incident laser which provides well-defined electron plasma waves. Thomson scattering of a short wavelength probe beam yields measurements of the amplitude of the waves resolved in time, space, wavelength and wavevector, that allow identification of the probed waves.

1 . Introduction

Stimulated Raman Scattering (SRS) is the decay of an electromagnetic wave (EMW) into another EMW and an electron plasma wave (EPW). SRS is important in the context of Inertial Confinement Fusion (ICF) because it can affect the propagation of the laser beams through the underdense plasma [1]. A significant part of the incident laser light can be reflected and the driven EPWs can produce hot electrons that preheat the fusion fuel and reduce the compression efficiency. According to linear theory of SRS, the daughter waves should grow exponentially in time to very high levels with a growth rate depending on the incident intensity. However, the characteristic growth time is short compared to the laser pulse duration so that SRS behavior is dominated by saturation processes. Consequently, the control of SRS in ICF experiments requires the identification of the saturation processes and the prediction of the saturation levels.

Theoretical work and numerical simulations [2] have suggested that the parametric decay of the EPWs driven by SRS can non linearly saturate the Raman instability by introducing an additional damping on the EPWs. The Langmuir decay instability (LDI) is the decay of a primary Langmuir wave into a secondary Langmuir wave and an ion acoustic wave (IAW). Recent experiments have shown the dependence of the SRS reflectivity on the IAW damping rate [3] as expected in the theoretical models of the saturation of SRS by LDI. EPWs travelling antiparallel to the laser wavevector have been observed [4] and were attributed to the LDI but some alternative explanations for the presence of such waves were proposed. Thus no clear experimental evidence of the LDI occurrence has been reported so far.

In this paper, we describe an experiment which allowed us to observe and identify the two LDI products as well as the EPW pump without any ambiguity. In section 2, the experimental set-up is presented. Sections 3 and 4 are devoted to the description of EPWs and IAWs produced by SRS and LDI. In section 5, features of collective Thomson scattering off a

2 . Experimental set-up

Five beams of the LULI (Laboratoire pour l'Utilisation des Lasers Intenses) facility were used to study the interaction between a 1.053 µm-wavelength laser beam, smoothed with a random phase plate (RPP), and a preformed underdense plasma. All beams were in the horizontal plane with 600 ps FWHM (full width at half maximum) Gaussian pulses. The plasma was formed by two counterpropagating 526 nm-wavelength laser beams ablating 1.2 µm thick, 380 µm diameter, CH disks and heated by a third, identical beam, delayed by 0.5 ns with respect to the first two. The plasma-forming beams were propagated through RPPs that produced a focal spot larger than the target, and the targets were sufficiently thin as to be completely transformed into a high-temperature plasma before the arrival of the interaction and probe laser beams. The interaction beam was focused along the principal axis of plasma expansion (normal to the target surface) and delayed by 1.4 ns with respect to the plasma formation pulses. Using an f/3 lens and an RPP consisting of a circular array of 2 mm elements, the focal spot diameter was 160 µm (FWHM), producing a peak intensity of $3.5\text{x}10^{14}$ W/cm^2. The Thomson scattering probe at 351 nm was synchronous with the interaction beam and was focused with a combination of a lens and an RPP with elongated elements to form a focal region 100 µm by 1 mm along the interaction beam axis, which was larger than the interaction region of interest. A parabolic mirror and two spherical mirrors collected scattered light and imaged the plasma on two spectrometers and streak cameras. This configuration yields Thomson scattering measurements resolved in time, space [5], wavelength and wavenumber. A layout of the beams and diagnostics is shown in *figure1.*

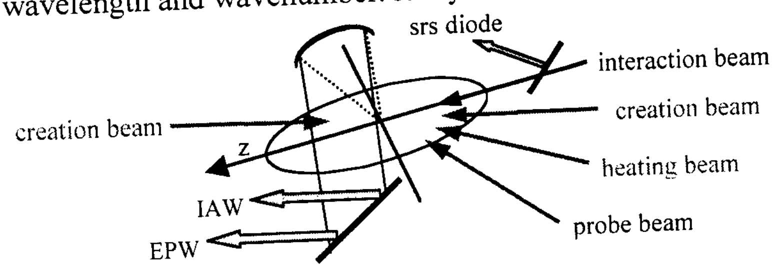

Figure 1: experimental set-up showing the Thomson scattering diagnostics (IAW, EPW) and the backscattered SRS detector.

3 . Stimulated Raman Scattering

SRS is a resonant three waves process where conservation laws for energy and momentum are satisfied: $\omega_0=\omega_{srs}+\omega_{epwl}$ and $k_0=k_{srs}+k_{epwl}$. These plasma normal modes also satisfy their dispersion relations: $\omega_0^2=\omega_{pe}^2+k_0^2c^2$, $\omega_{srs}^2=\omega_{pe}^2+k_{srs}^2c^2$, $\omega_{epwl}^2=\omega_{pe}^2+3k_{epwl}^2v_{the}^2$. If we neglect the Bohm-Gross correction in this latter relation, norms of the wavevectors for both electromagnetic waves are depending only on the electron density and we find: $k_0=(\omega_0/c)(1-n_e/n_c)^{1/2}$ and $k_{srs}=(\omega_0/c)[(1-2(n_e/n_c)^{1/2}]^{1/2}$. Since k_0 is also known in direction, $k_0=k_{srs}+k_{epwl}$ shows that the extremity of k_{srs} is on a circle of radius k_{srs}, with its center at one extremity of k_0 as shown in *Figure 2.*

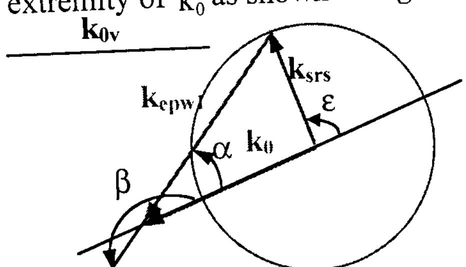

Figure 2: diagram of the wavevectors in the SRS decomposition. $k_{0v}=\omega_0/c$ is the wavevector of the incident laser light in the vacuum. The amplitude of the wavevectors has been calculated for $n_e/n_c= 0.1$.

For stimulated Raman backscattering, $k_{epwl}=k_0+k_{srs}$ is a decreasing function of the

$1.72\omega_0/c$ and $1.22\omega_0/c$ in this range. In the case of sidescattering, k_{epw1} is calculated as a function of ε and n_e/n_c as follow: $k_{epw1}=k_0-k_{srs}$ => $k_{epw1}^2=k_0^2+k_{srs}^2+2k_0k_{srs}\cos(\varepsilon)$. Direction of the stimulated EPW is referenced with respect to the interaction beam axis by the angle β ($=\alpha+\pi$). Then α is deduced from: $k_{srs}=k_0-k_{epw1}$ => $k_{srs}^2=k_0^2+k_{epw1}^2-2k_0k_{epw1}\cos(\alpha)$.

4 . Langmuir Decay Instability

The electron plasma waves and the ion acoustic wave involved in the LDI process follow relations of the same type than in the SRS process: $\omega_{epw1}=\omega_{epw2}+\omega_{iaw2}$ and $k_{epw1}=k_{epw2}+k_{iaw2}$. In the following discussion, we will consider LDI backscattering only so that EPW2 and IAW2 have the same direction than the SRS driven EPW (EPW1). The dispersion relation for the ion acoustic wave is: $\omega_{iaw2}=k_{iaw2}c_s$. Assuming $k_{epw1,2}<< k_D=1/\lambda_{De}$ which is satisfied as long as Landau damping of the Langmuir waves is negligible, characteristics of the daughter waves can be calculated as a function of k_{epw1}: $k_{epw2}=-k_{epw1}+\Delta k$ and $k_{iaw2}=2k_{epw1}-\Delta k$ where $\Delta k = (2/3)\, k_D\, (Zm_e/m_i)^{1/2}\# \,(n_e/T_e)^{1/2}$ for a homogeneous plasma [6]. For $n_e/n_c=0.1$ and $T_e=500$ eV, we calculate $\Delta k=0.11\omega_0/c$ which is only a few percents of k_{epw1}.

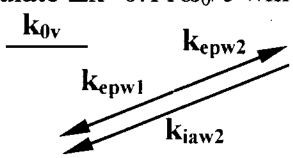

Figure 3: schematic of the LDI. Features of the SRS driven EPW, k_{epw1} in length and direction, can be calculated as a function of ε and n_e/n_c. The same informations for k_{epw2} and k_{iaw2} are straightforward.

5 . Thomson scattering geometry

Collective Thomson scattering off a coherent wave [7] (produced by a stimulated scattering instability) is a resonant process in which wavevectors and pulsations of the probe (k_p,ω_p), scattered light (k_s,ω_s) and plasma wave $(k_{iaw,epw},\omega_{iaw,epw})$ (iaw or epw) must satisfy: $\omega_s=\omega_p\pm\omega_{iaw,epw}$ and $k_s=k_p\pm k_{iaw,epw}$. For given plasma wave and probe beam wavevectors, the scattered light is emitted in two directions and its spectral characteristics result from the previous laws. Respectively, when the direction of observation (k_s) is fixed, the probed plasma wave is determined by: $k_{iaw,epw}=\pm(k_p-k_s)$ which corresponds, in the case of IAWs, to two counterpropagating wavevectors.

Nature of the probed plasma wave determines further details in the Thomson scattering geometry. For IAWs, one has: $\omega_{iaw}<<\omega_p$, ω_s and can write $\omega_p\approx\omega_s$ which involves, using the dispersion relation for the electromagnetic waves, that the probe and scattered light wavevectors have approximately the same length: $k_p=(\omega_0/c)(9-n_e/n_c)^{1/2}$. In *figure 4*, a schematic of the scattering is considered in two different cases. *Figure 4a* represents the case where the IAW we want to probe is known as well as the probe beam wavelength. The isosceles triangle can be built in two ways leading to scattered light emitted in two directions with a characteristic pulsation for each direction: $\omega_{sup}=\omega_{pup}+\omega_{iaw}$ for $k_{sup}=k_{pup}+k_{iaw}$ and $\omega_{sdown}=\omega_{pdown}-\omega_{iaw}$ for $k_{sdown}=k_{pdown}-k_{iaw}$. Another triangle may be drawn by a symmetry of the previous one with respect to the IAW but the probe and scattered light would be far from our experimental geometry in this case. *Figure 4b* considers the case where the probe and scattered light of given wavelength, have a wavevector well-defined in direction. Then two well-defined counterpropagating IAWs are probed and the pulsation of the scattered light is given by the direction of propagation of the corresponding IAW. In the case of Thomson scattering off EPWs, the probe and scattered light wavevectors have different lengths. For the down scattered light: $\omega_{sdown}^2=\omega_{pe}^2+k_{sdown}^2c^2=\omega_p^2-2\omega_{epw}\omega_p+\omega_{epw}^2$ gives $k_{sdown}=(\omega_0/c)[9-6(n_e/n_c)^{1/2}]^{1/2}$. For the up scattered light, we find the same way:

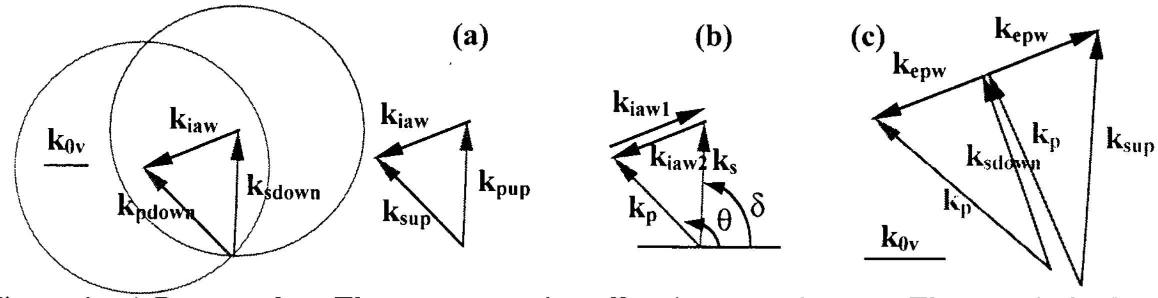

Figure 4: a) Down and up Thomson scattering off an ion acoustic wave. The two circles have a radius equal to k_p and their centers are the extremities of k_{iaw}. Wavevector dimensions have been calculated for n_e/n_c= 0.1. Scales are different in figures 3a and 3c and the corresponding lengths for k_{0v} are indicated in each case. b) IAWs probed for given probe and scattered light wavevectors. c) up and down Thomson scattering off two counterpropagating EPWs.

We are interested here with the observation of the plasma waves involved in LDI, for which we know all the characteristics: direction and wavenumber. Experimental constraints limit the possibilities. The angle of the probe beam (θ) is between 125° and 145° and the collection optics limits the scattering angle (δ) in the range [74°;118°] (see *figure 4b* for a definition of θ and δ). It is clear from *figure 4* that the only possibility is to collect down Thomson scattered light off IAW2 and EPW1 and up scattered light off EPW2. Then Thomson scattering triangles are known and one can calculate all the angles of interest: amplitudes of the wavevectors are given as a function of the electron density then θ and δ are calculated as for the calculation of α in the SRS description. The results are shown in *figure 5* for Thomson scattering off IAW2.

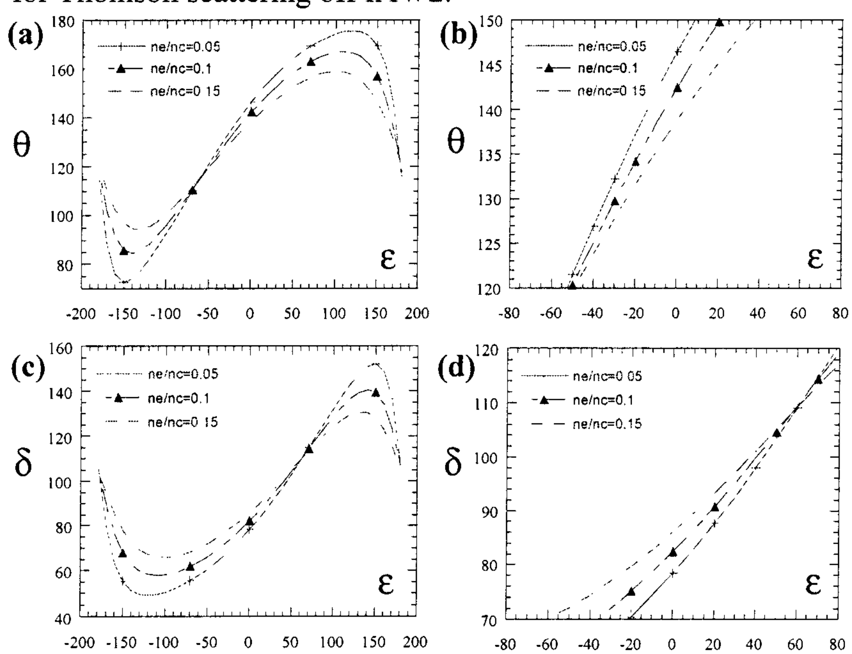

Figure 5: a) probe angle (θ) used for Thomson scattering off IAW2 as a function of the characteristic angle of the SRS decomposition (ε) for different values of n_e/n_c; b) detail of the previous graph in the range of interest; c) resulting scattered light angle (δ); d) detail for the collection angles available in the experiment.

In the experiment, we used masks inside the probe and collection apertures in order to observe well-defined IAWs. Selecting δ=[79°;84°] and θ=[141°;145.5°], we probed IAWs corresponding to the decay of EPW1 driven by SRS backscattering (see *figure 5*). By doing so, we can only observe two counterpropagating IAWs whose wavevectors are well-defined (see *figure 4b*). A plot of the observed signal is shown in *figure 6.* The IAWs spectrum exhibits two components (IAW2 and IAW3) separated by 4.1Å. This separation is equal to $2\lambda_p c_s k_{iaw2}/k_p$ for the probed IAW and the measured electron temperature (0.7 keV). The IAW3 peak corresponds to an IAW with $\vec{k}_{iaw3}=-\vec{k}_{iaw2}$ and is the product of the LDI of EPW2.

by similar formulas. In *figure 7,* Thomson scattering signals from EPW1 and EPW2 have been plotted as a function of the scattered wavelength. *Figures 7 c* and *d* correspond to a later time (90 ps later) during SRS than *figures 7 a* and *b.* Since $\omega_{epw1,2}$ is proportional to the square root of n_e/n_c, the evolution of the peaks in λ seen in *figure 7* are consistent with the relations $\omega_{sepw1}=\omega_p-\omega_{epw1}$ and $\omega_{sepw2}=\omega_p+\omega_{epw2}$ when the density is decreasing during the interaction because of the plasma expansion. Thomson scattering off EPWs resolved in time, space and wavelength can be used as a density diagnostic.

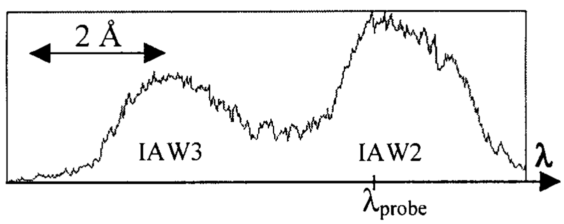

Figure 6: plot of the Thomson scattered light off IAWs as observed with the masks δ=[79°;84°] and θ=[141°;145.5°]. The IAW2 peak has the expected characteristics of the LDI product of EPW1 decay whereas the IAW3 peak is the result of Thomson scattering off an IAW propagating in the opposite direction to IAW2.

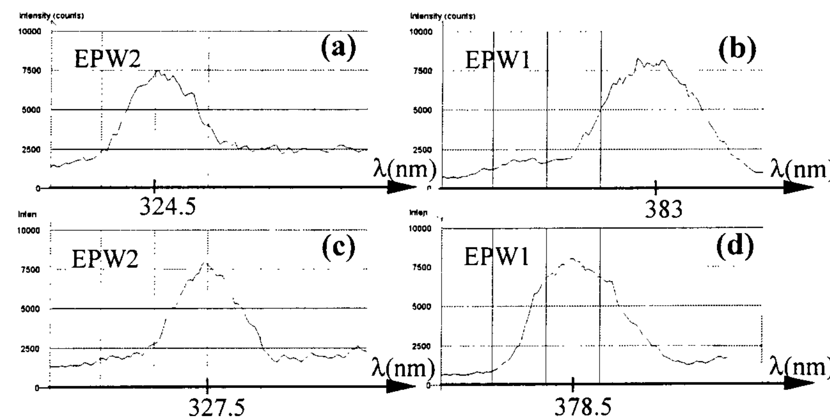

Figure 7: plots of the Thomson scattered light off EPWs corresponding to EPW1 and EPW2 as a function of wavelength for two times during the SRS occurrence. The signal is integrated over 50 ps for each plot.

In summary, design and geometry of the Thomson scattering diagnostics used in this experiment have been described. Using this diagnostic, we have observed and identified EPWs and IAWs having the expected spectral characteristics for the LDI products of the SRS driven EPW. This is the first demonstration of the occurrence of LDI in laser-plasma experiments.

The authors gratefully acknowledge the support of the technical groups of LULI. This work was partially supported under the auspices of the U.S. Department of Energy by the Lawrence Livermore National Laboratory under contract No.W-7405-ENG-48. Part of this support was provided through the LLNL-LDRD program under the Institute for Laser Science and Applications.

References

[1] W. L. Kruer, *The Physics of Laser plasma Interactions* (Addison Wesley Publishing Co., Redwood City, CA, 1988) ; H.A Baldis, E.M. Campbell, and W.L. Kruer, "Laser-plasma interactions", in *Physics of Laser Plasmas,* Handbook of Plasma Physics, North-Holland, Amsterdam 1991, p.361-434 ; D. Pesme, C. Labaune "La Fusion Thermonucléaire Inertielle par Laser", vol. 1, R. Dautray, J-P Watteau, editors, Eyrolles, Paris (1993).

[2] S.J. Karttunen, Phys. Rev. A **23**, 2006 (1980) ; J.A. Heikkinen and S.J. Karttunen, Phys. Fluids **29**, 1291 (1986) ; T. Kolber, W. Rozmus, and V.T. Tikhonchuk, Phys. Fluids B**5**, 138 (1993) ; B. Bezzerides, D.F. DuBois, and H.A. Rose, Phys. Rev. Lett. **70**, 2569 (1993) ; D.A. Russell, D.F DuBois, and H.A. Rose, Phys. Plasmas **6**, 1294 (1999) ; D.F DuBois, H.A. Rose, and D.A. Russell, Phys. Sci. **T63**, 16 (1996) ; R.L. Berger, C.H. Still, E.A. Williams, and A.B. Langdon, Phys. Plasmas **5**, 4337 (1998).

[3] J. C. Fernández *et al.,* PRL **77**, 2702(1996); R. K. Kirkwood *et al.,* PRL **77**, 2702(1996); D.S. Montgomery *et al.,*Phys. Plasmas **5**, 1973(1998).

[4] C. Labaune, H.A. Baldis, B.S. Bauer, V.T. Tikhonchuk, and G. Laval, Phys. Plasmas **5**,234(1998); K.L. Baker *et al.,* PRL 77, 67(1996)

[5] H.A. Baldis and C. Labaune, Rev. Sci. Instr, **67**, 451 (1996).

[6] V.N. Oraevskii and R.Z. Sagdeev, Sov. Phys. Tech. Phys. 7, 955 (1963)